Integrating-sphere system and method for absolute measurement of transmittance, reflectance, and absorptance of specular samples

Leonard Hanssen

An integrating-sphere system has been designed and constructed for multiple optical properties measurement in the IR spectral range. In particular, for specular samples, the absolute transmittance and reflectance can be measured directly with high accuracy and the absorptance can be obtained from these by simple calculation. These properties are measured with a Fourier transform spectrophotometer for several samples of both opaque and transmitting materials. The expanded uncertainties of the measurements are shown to be less than 0.003 (absolute) over most of the detector-limited working spectral range of 2 to 18 μm. The sphere is manipulated by means of two rotation stages that enable the ports on the sphere to be rearranged in any orientation relative to the input beam. Although the sphere system is used for infrared spectral measurements, the measurement method, design principles, and features are generally applicable to other wavelengths as well. © 2001 Optical Society of America

OCIS codes: 120.0120, 120.3150, 120.5700, 120.7000, 120.3940, 120.4570.

1. Introduction

Integrating spheres have long been used for the measurement of diffuse reflectance and transmittance of materials in the UV, visible, and near-IR spectral regions, as well as somewhat more recently (since the 1970's) in the mid- to far-IR regions. However, integrating spheres have been used infrequently for specifically measuring specular materials. This is true despite the fact that, according to integrating-sphere theory, for an ideal sphere, a simple ratio of two measurements should result in the absolute reflectance of a specular sample. The reason for the lack of use of integrating spheres for specular measurements of reflectance is that real integrating spheres are not ideal. The sphere-wall coating is never a perfect Lambertian diffuser, baffles perturb the light distribution within the sphere, and all detectors exhibit some angular dependence. These and other deviations from an ideal sphere can drastically affect the accuracy of the sphere equations.[1]

Because of the deviations, all spheres have some degree of nonuniformity of throughput. This means that the detector signal will vary as the direction of the reflected or the transmitted light (and the regions upon which the light is incident) within the sphere is varied. The result may be errors in the quantities derived from the measurements. For this reason, measurements of reflectance of specular materials are usually performed relative to a known specular standard. When this is done, the regions of the sphere wall upon which the reflected light of the sample and the reference falls usually have similar throughputs.

For absolute regular (specular) reflectance measurements, various methods, including, V–W, V–N, and goniometer-based methods, are typically used.[2,3] These methods typically do not involve an integrating sphere. They involve an input beam, several directing mirrors, and the detector. Some subsets of the mirrors, the sample, and the detector are rotated and translated between sample and reference measurements. For the V–N and the goniometer methods, a simple ratio of the two results produces the absolute sample reflectance, whereas for the V–W method, the square root is taken.

The primary sources of error in the methods just mentioned are the result of alignment problems and the spatial nonuniformity of the detector. These problems can easily lead to errors of several percent

L. Hanssen (hanssen@nist.gov) is with the Optical Technology Division, National Institute of Standards and Technology, Gaithersburg, Maryland 20899.

Received 17 October 2000; revised manuscript received 20 March 2001.

0003-6935/01/193196-09$15.00/0

© 2001 Optical Society of America

or more.[4] With considerable effort to achieve accurate alignment, excellent results can be achieved for standards quality samples. However, even in these cases, characteristics of the sample surface can limit ultimate measurement accuracy.[5,6] For transparent materials, dealing properly with the transmitted light and measuring the backsurface reflection accurately pose additional difficulties.

An important application of integrating spheres is their use as an averaging device for detectors. Because of the useful properties of the sphere, an averaging sphere's entrance port can be both significantly larger and much more spatially uniform than a bare detector. The trade-off made for these improvements is a degradation of the signal-to-noise ratio. The benefits of using the integrating sphere for more accurate detection of light are used in the design of the system and development of the method presented in this paper. The measurement of absolute transmittance (τ), reflectance (ρ), and absorptance (α) of specular samples is described and demonstrated. The inherent problems of sphere spatial nonuniformity are overcome through judicious use of the symmetries of the sphere design to establish symmetries in the measurement geometry. After describing the specifics of the integrating sphere in Section 2, the other components of the sphere system in Section 3, and the absolute measurement method in Section 4, we present the sphere characterization measurement results for error analysis in Section 5. The achievement of measurement uncertainties of 0.002 to 0.004 are demonstrated in Section 6 for several common IR materials. Finally, Section 7 contains the discussion of the results with conclusions about the usefulness of the sphere method for specular materials.

2. Description of the Integrating Sphere

The integrating-sphere system has been designed and constructed according to the specifications detailed in the following paragraphs. Figure 1 is a photograph of the integrating sphere. Specific parameters of the sphere, including a description and analysis of the detector–nonimaging-concentrator system, have been described previously.[7] The inside wall of the sphere is coated with a material that is nearly a Lambertian diffuser and at the same time has a high directional hemispherical (diffuse) reflectance ($\geq$0.9) for the IR spectral range: plasma-sprayed Cu on a brass substrate, electroplated with Au.

The sphere has entrance, sample, and reference ports, all centered on a great circle of the sphere, as shown in Fig. 2. There also is a detector port, with its center located along the normal to the great circle. The white Hg:Cd:Te (MCT) detector Dewar located on the port can be seen mounted on the top of the sphere in Figs. 1 and 2. The detector's field of view is centered on the same normal and corresponds to the bottom region of the sphere. The sample and the reference ports are located symmetrically with respect to the entrance port and can be seen in the foreground of Fig. 1 (the sample port has a KRS-5 sample mounted on it). The exact location of the sample and the reference ports is in general determined by the angle of incidence for which the reflectance and the transmittance are to be determined. An arrangement of ports could, in principle, be set up for any angle of incidence from approximately 2° to 28° and from 32° to 75°, depending on the input-beam geometry of the source (or spectrophotometer). For this sphere, port locations have been selected for 8°, which is close to normal incidence, yet for which no portion of the $f/5$ (6° half-angle) input beam will be reflected back onto itself. (For incidence angles in the neighborhood of 30°, a variation of the design would be required so that the reflected beam from the sample port does not hit the reference port and vice versa). The entrance port is of sufficient size (3.3-cm diameter) to accept the entire input beam, and the sample and the reference ports are also sized (2.22-cm diameter) to accept the entire beam (at the focus, in a focused geometry). All the ports are circular in shape, with the sphere's inside and outside surfaces forming a knife edge at the port edge where they meet. In this sphere, as seen in Fig. 2, the measurement of reflectance is designed for an incidence angle of 8° (in general θ); the sample and the reference ports are located at 16° (in general $+2\theta$) and $-16°$ (in general -2θ), respectively, measured from the center of the sphere and with respect to the line through the sphere center and the sphere wall (at

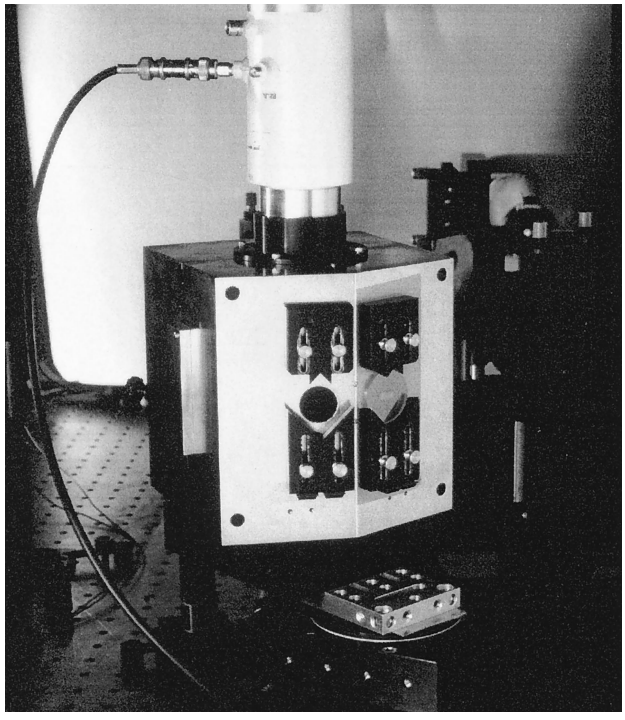

Fig. 1. Photograph of the integrating sphere for absolute IR spectral transmittance and reflectance. The Hg:Cd:Te (MCT) detector Dewar (white) is mounted on the top of the sphere. We view the back side of the sphere that includes reference (empty) and sample (with a KRS-5 window) ports. A pair of rotation stages underneath the sphere is used to move the sphere into positions for both reflectance and transmittance measurements.

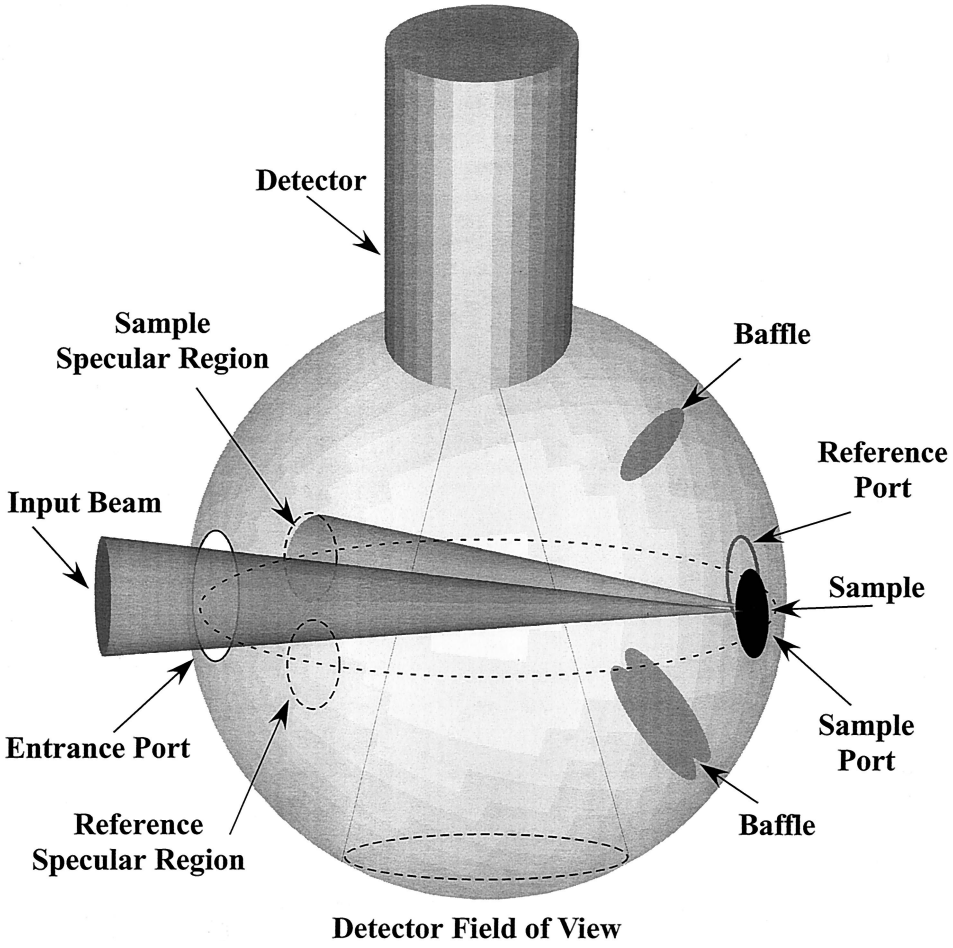

Fig. 2. Diagram of sphere interior and arrangement of its elements. Input and reflected beams are shown for a specular sample in the reflectance measurement geometry. The sample and the reference specular regions of the sphere wall are the first to be illuminated in the sample and the reference measurements, respectively. The baffles are positioned for measurement of diffuse samples and are not critical for specular sample measurement.

a point directly opposite the entrance port). Baffles separating the detector port and the detector field-of-view region from the sample and the reference ports are shown in Fig. 2. The baffles are critical to the sphere performance for characterization of diffuse samples,[8] but do not play a significant role for the specular-sample case.

The arrangement of the ports described above results in the regions of the sphere wall illuminated by the specularly reflected or transmitted light and the reference beam being centered on the same great circle as the entrance, sample, and reference ports. In addition, the regions are symmetrically positioned around the entrance port. The reflected or the transmitted light also will be incident at the same angle on these regions. As a result, the reflected or the transmitted light will have throughput to the detector that is nearly identical. The procedure for orienting the sphere for the reflectance, transmittance, and reference measurements is described in Section 3.

3. Sphere Mounting and Manipulation Hardware

The sample and the reference mounts, a pair of which can be seen on the sphere in Fig. 1, are constructed to hold the sample against and centered on the sample port from outside of the sphere. During sphere movement, the holders prevent the sample from moving or shifting relative to the sample port. This is done in such a way as to leave the back of the sample free and open, so that the beam centered on the sample can proceed through it (for a transparent sample) without obstruction. This is required for performing either transmittance or reflectance measurements on transparent samples. This arrangement can also be used to check thin-film mirrors for optical opacity.

The integrating-sphere system includes two motorized rotation stages stacked on top of each other. The stages are mounted with their axes of rotation parallel to each other. The rotation axes of the stages are identified in Fig. 3. Stage 1 has its axis of rotation oriented parallel to the normal of the great circle formed by the entrance-, sample-, and detector-port centers, as well as passing through the edge of this circle. This base stage remains fixed to the optical table. Its rotation axis is perpendicular to the input beam and passes through the beam-focus position. Stage 2 is mounted on the rotation table of the base stage so that its axis of rotation is located a distance

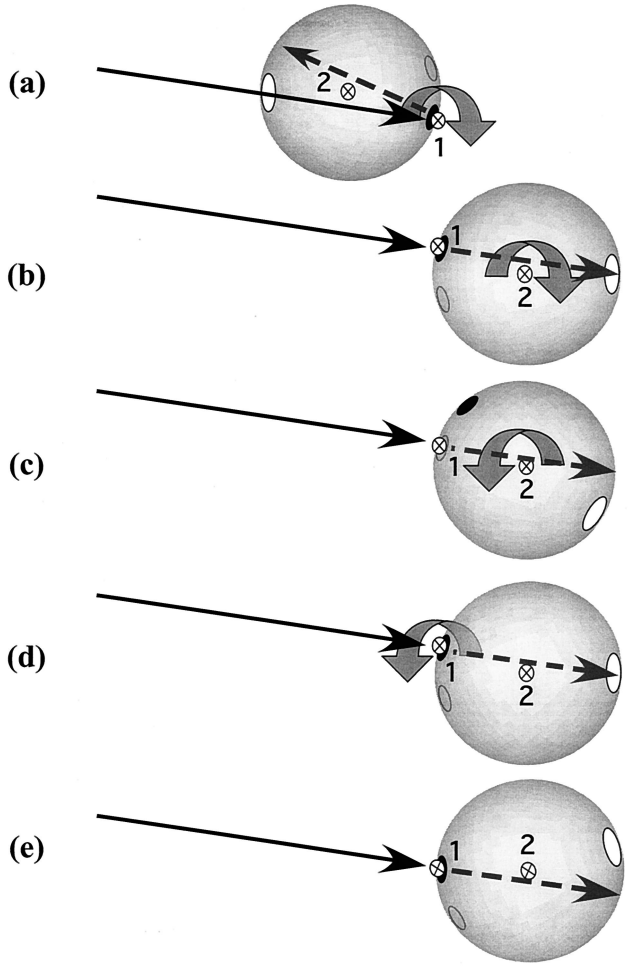

Fig. 3. Sphere measurement geometries for reflectance and transmittance and rotation steps used to orient the sphere for each (a) reflectance measurement geometry, (c) reference measurement, and (e) transmittance measurement geometry. (b) and (d) are intermediate steps. Two rotation stages, stage 1 centered at the input-beam focus and sphere wall and stage 2 centered at the sphere center, are used to change geometries.

away from the base-stage axis exactly equal to the sphere radius. The integrating sphere is mounted to the rotation table of stage 2 so that the stage's axis of rotation is along the sphere axis that includes the center of the detector port and the sphere center.

The function of base stage 1 is to vary the angle of incidence of the input beam on the sphere surface and to switch between reflectance and transmittance measurement geometries. The function of stage 2 is to select upon which port, the entrance, the sample, or the reference port, the beam will be incident.

4. Measurement Geometry and Method for Reflectance and Transmittance

The arrangement of the input beam and the integrating sphere for absolute transmittance and reflectance measurements is shown in Fig. 3. The sample reflectance measurement setup is shown in Fig. 3(a) (as well as in Fig. 2), the reference measurement in Fig. 3(c), and the sample transmittance measurement in Fig. 3(e). In each diagram, the rotation required for reaching the following diagram is shown as a curved arrow around the appropriate rotation axis. In the reflectance measurement geometry of Fig. 3(a), the input beam passes from the spectrometer through the sphere entrance port and onto the sample surface facing the sphere. This is the typical reflectance geometry for directional-hemispherical sample reflectance in most sphere systems. The only difference in Fig. 3(a) is the empty reference port (as opposed to one occupied with a standard for a relative measurement). On reflection off the sample, the beam transverses the sphere and is incident upon a region we denote as the sample specular region (see Fig. 2). From this point, the reflected flux is distributed throughout the sphere in an even fashion because of the Lambertian coating and the integrating nature of the sphere. In Fig. 3(a) a clockwise rotation about axis 1 turns the back of the sample to the beam in Fig. 3(b). An additional clockwise rotation about axis 2 places the (empty) reference port at the input beam focus in Fig. 3(c), where it continues on to strike the sphere wall at the reference specular region (labeled in Fig. 2), producing the reference measurement. Another counterclockwise rotation about axis 2 results in Fig. 3(d), a repeat of Fig. 3(b). A final counterclockwise rotation about axis 1 positions the sphere in Fig. 3(e) for the transmittance measurement, with the same angle of incidence as that of Fig. 3(a) on the sample and incidence region on the sphere wall (the sample specular region).

The somewhat unusual geometry for the reference measurement [Fig. 3(c)] is chosen in order to achieve the highest degree of symmetry between the reflectance and the reference measurements. The sample and the reference specular regions are symmetrically located on either side of the entrance port. Because of the symmetry of the sphere design, the throughput is nearly equal for these two regions. Because the only other difference between the sample reflectance and reference measurements is the initial reflection off the sample, the ratio of sample reflectance and reference measurements is equal to the absolute sample reflectance (for specular samples). Various sources of error, including the difference in the sample and the reference specular region throughputs, can be included in the expanded measurement uncertainty or can be corrected for.

The ratio of the sample reflectance measurement of Fig. 3(a) to the reference measurement of Fig. 3(c) is equal to the absolute sample reflectance (for specular samples). The ratio of the transmittance measurement of Fig. 3(e) to the reference measurement of Fig. 3(c) is equal to the absolute sample transmittance (for specular samples).

The absolute absorptance is indirectly obtained when the sum of the absolute reflectance and transmittance is subtracted from unity. Kirchoff's law applies because the reflectance and the transmittance measurements are made under identical conditions of geometry and wavelength(s). The input beam is incident upon opposite surfaces of a sample

for the reflectance and the transmittance measurements. For a uniform sample with identical front and back surfaces, the side of incidence is immaterial. For samples with some asymmetry that is due to, for example, a coating on one or both sides, the sample can be reversed to make a pair of reflectance measurements and to obtain the corresponding pair of absorptance results.

5. Measurement Conditions and Sphere Characterization

The integrating-sphere system is a measurement component of a larger Fourier transform (FT) spectrophotometer (FTS) system described in more detail elsewhere.[9] The incident-beam geometry for all measurements described in Sections 5 and 6 is an $f/5$ cone with an 8° central angle of incidence. The FTS was configured with a W–halogen lamp and coated-quartz beam splitter for the near-IR spectral region of 1 to 3 μm (10,000 to 3300 cm^{-1}), and a SiC source and coated-KBr beam splitter for the mid-IR region of 2 to 18 μm (5000 to 550 cm^{-1}). The spectral resolution is either 4 or 8 cm^{-1} for all results shown.

Every plot of transmittance and reflectance is obtained by the following procedure. A number of alternating measurements of reference, sample reflectance, and sample transmittance (where appropriate) single-beam spectra are performed according to Fig. 3 and are repeated between 8 and 24 times. For each repetition, we calculate the transmittance and the reflectance by taking ratios of the corresponding single-beam spectra and a reference single-beam spectrum (obtained by interpolation to reduce the error that is due to instrumental drift). From the resulting series of individual transmittance and reflectance spectra, the mean transmittance (τ) and reflectance (ρ), along with the standard deviation and standard error, spectra are calculated. Finally, the absorptance spectrum is obtained from $1 - \tau - \rho$.

We obtain each single-beam spectrum by coadding 512 or 1024 scans of the FTS. The total measurement time for most of the results shown is several hours (from 2 to 10). The long measurement times are required for obtaining the lowest noise level in the spectra. For less stringent requirements of 1% uncertainty, shorter measurement times of the order of 10 to 20 min will suffice.

In addition to the various potential sources of error that are due to the FT spectrometer,[10,11] several other sources of error may play a role in the sphere system measurements. These are (1) spatial nonuniformity of the sphere-wall regions directly illuminated by the input beam (reference specular region) or sample first reflection (sample specular region), (2) nonuniformity of the throughput of the sphere-wall region directly illuminated by the input beam compared with that of the region illuminated by the sample first reflection; (3) overfilling the entrance port in the sample reflectance measurement, and (4) overfilling the sample port in any of the measurements.

The spatial nonuniformity of the integrating-sphere throughput has been evaluated at the 10.6-μm wavelength by use of a CO_2 laser system. The local spatial variation across the region illuminated directly by the reference beam or indirectly by a specularly reflected or transmitted beam is approximately ±0.4%.[8] A translation of the light incident upon the sphere wall of 0.5 cm through deflection or deviation (of 2°) should result in a ±0.1% relative change in throughput. Thus a transmittance measurement of a sample with an effective wedge of 1° could lead to a 0.1% relative error in transmittance. Because of the decrease in wall reflectance and corresponding decrease in throughput with decreasing wavelength, the error that is due to spatial nonuniformity is greater at shorter wavelengths, especially in the near-IR region, approaching 1 μm.[9] Spectral evaluation of this error is currently in progress.

The difference in throughput between sample- and reference-port measurement geometries can lead to a small relative error, varying between 0% and 0.5%, depending on wavelength. The direct measurement of transmittance or reflectance for specular samples will include this error, but an additional measurement of the transmittance ratio of empty sample and reference ports can be used to correct for the error. This has been done with good reproducibility and need not be repeated unless the optical-input-system geometry or alignment is altered. A plot of such a throughput ratio is shown in Fig. 4.

Besides the generally featureless spectral curve, a sharp structure occurs at approximately 8.5 μm. This structure occurs at the only wavelength at which the incident beam from the FTIR beam is significantly polarized. It is anticipated that a future test of the sphere in which polarized light is used will show increased throughput variation with polarization. At the same time, averaging *s*- and *p*-polarized beam measurements is expected to eliminate the structure seen at 8.5 μm.

The extent of overfilling the entrance, sample, and reference ports can be examined by a measurement of an empty sample or reference port in the reflectance mode. Any light coming through the entrance port and overfilling the sample (or reference) port will be measured as a reflectance component with near-unity reflectance of the sphere-wall region surrounding the port. In addition, any overfilling of the entrance port in that measurement will result in some light scattering off the rim of the entrance port into the sphere, resulting also in a reflectance component with high effective reflectance. A knife-edge design could be used to reduce the result of entrance-port overfilling, but it is preferable to be sensitive to it in order to quantify it (set an upper limit to it). An example of the combined overfilling-error reflectance measurement is shown in Fig. 5. This was obtained after careful alignment of the sphere system and the input FTIR beam. The level of this measurement is lower than has been reported previously.[9] The previous empty-port measurement was in error because of a subtlety of the FT processing that produced a rectification of the noise in the measurement. This error was eliminated when the phase-error spectrum

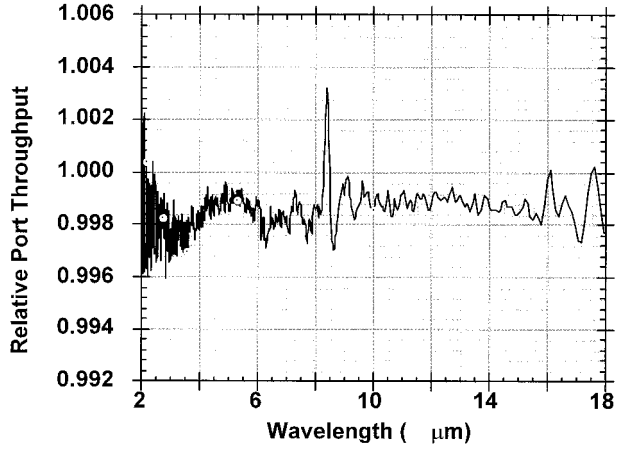

Fig. 4. Sample- and reference-port throughput comparison, the result of an empty-sample-port transmittance measurement. The curve represents the difference in detector signal for specularly transmitted and reflected light from the sample compared with light in the reference case. This spectrum can be used in either of two ways: (1) as a component to the systematic uncertainty of ρ or τ, or (2) as a correction spectrum to divide into the initially obtained spectra of ρ or τ to eliminate the error.

obtained in the reference measurement was used for correction of the sample empty-port measurement.

The remaining important sources of error are related to the FTIR spectrometer, detector, electronics, and FT processing, which are not discussed in detail here. The combined measurement error for the transmittance and the reflectance measurements include both FTIR-related errors and the integrating-sphere system errors. A straightforward method of evaluating the measurement accuracy of the system is to compare measurement results with calculated results for the optical properties of common IR optical materials. Measurements of a few common materials are presented in Section 6, and the results are used to perform this comparison.

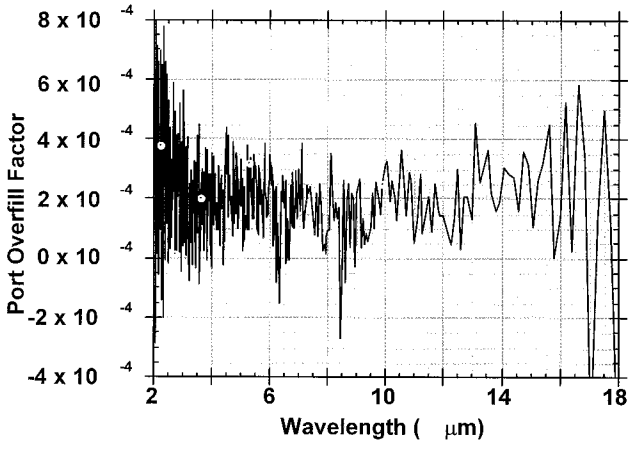

Fig. 5. Sample-port overfill measurement, the result of an empty-sample-port reflectance measurement. This is a characterization of the baseline measurement capability of the integrating-sphere system. The result can be used to apply corrections to a black sample measurement.

6. Transmittance, Reflectance, and Absorptance Results

A number of optical components have been characterized by the integrating-sphere system, including windows, filters, and mirrors. Several examples of window materials are shown in Figs. 6 and 7. Both transmittance and reflectance are measured with the same geometry. From these two quantities the absorptance is simply determined by subtraction of their sum from 1. Comparisons can be made with calculated values from handbook indexes of refraction data.[12,13] This can be done in two ways: (1) A comparison can be made with calculated transmittance and reflectance, and (2) a comparison can be made with calculated absorptance.

The calculated τ and ρ values from the n and k values in handbooks have finite uncertainty values. These are based on the uncertainties of the original data and the mathematical processes with which the index values n and k were obtained. Other sources of error in this comparison include variations in the material itself, such as the method of growth and processing.

For specific spectral regions for many materials, however, the calculated absorptance can be determined, with insignificant ($<10^{-4}$) error, to be 0. Because of this, the indirectly measured absorptance in these spectral regions can be used as an accurate evaluation of the total measurement error, not just as an estimate of uncertainty. If, in addition, a number of materials with transmittance and reflectance values spanning a significant fraction of their range (0 to 1) are measured, the measurement error can then be used with reasonable confidence for all transmittance and reflectance results.

Four common IR window materials were characterized with the sphere system, with the results plotted in Figs. 6(a)–6(d). They are Si (0.5 mm thick) [Fig. 6(a)], ZnSe (3 mm thick) [Fig. 6(b)], KRS-5 (5 mm thick) [Fig. 6(c)], and MgF_2 (5 mm thick) [Fig. 6(d)]. For each sample, the transmittance, reflectance, and absorptance are plotted over a spectral range of 2–18 μm [1–18 μm for Fig. 6(a)]. Each material has a nonabsorbing spectral region over some portion of that range. The reflectance values (in the nonabsorbing range) for the selected materials range from 0.05 to 0.45, and the corresponding transmittance values range from 0.55 to 0.95, in the nonabsorbing regions. The MgF_2 spectrum exhibits a wide range of values for ρ, τ, and α within the spectral range. At 12.5 μm, both the reflectance and the transmittance are 0, at which the absorption coefficient is substantial ($\tau \rightarrow 0$) and the index n is close to 1 ($\rho \rightarrow 0$).

A closer examination of the indirectly measured absorptance in the nonabsorbing regions is shown in Figs. 7(a)–7(d). For each material, an absorptance close to 0 is observed in the spectral regions with a nearly 0 k value. These are 1.2–5.5 μm [Fig. 7(a)], 2–13.5 μm [Fig. 7(b)], 2–18 μm [Fig. 7(c)], and 2–4.5 μm [Fig. 7(d)]. In the results,

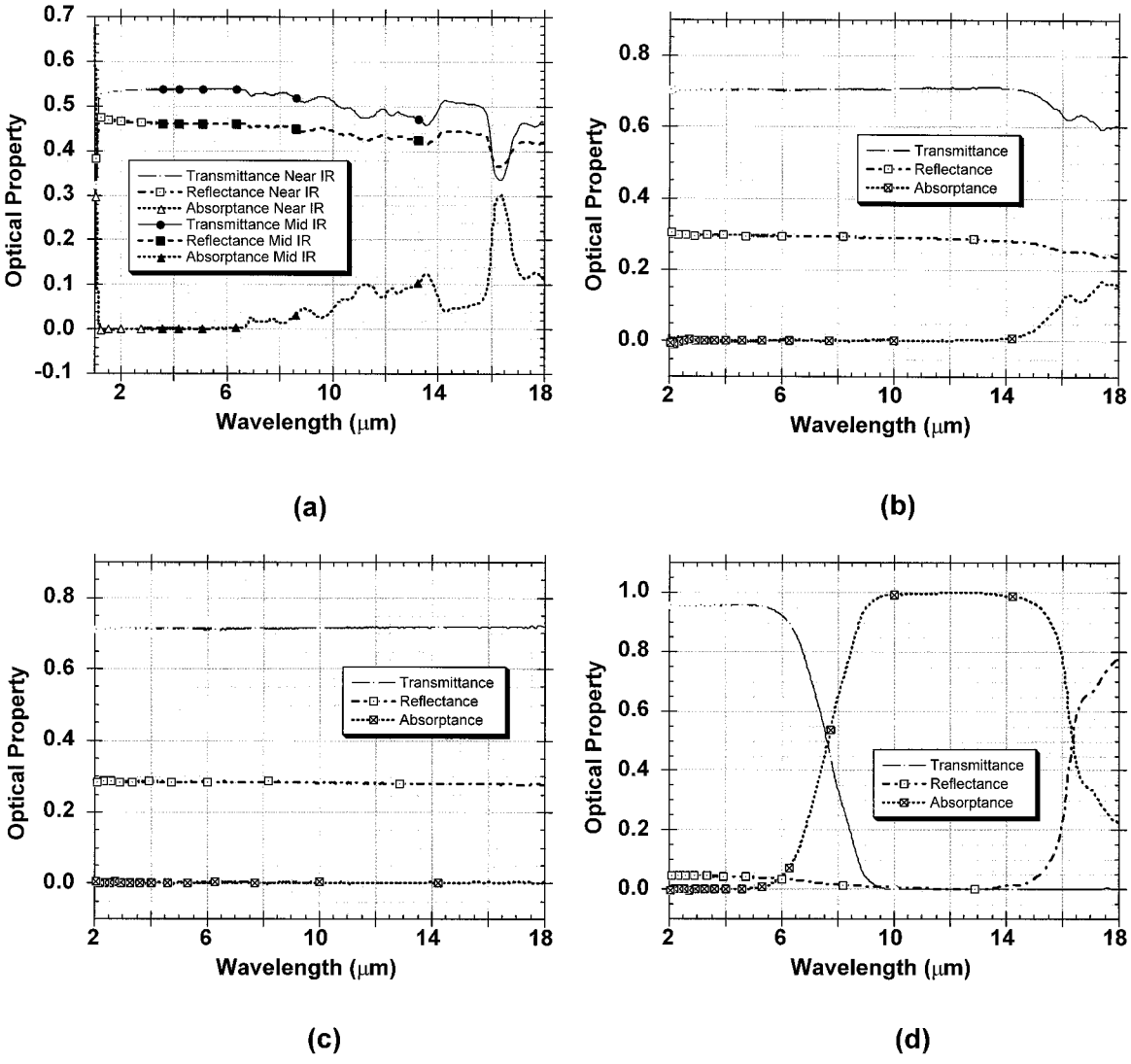

Fig. 6. Transmittance, reflectance, and absorptance (obtained from $1 - \rho - \tau$) of several common IR window materials, ranging in index from 3.4 to 1.3: (a) Si, (b) ZnSe, (c) KRS-5, (d) MgF_2.

spectral features are seen that can be attributed to contaminants, primarily on the surface, such as water and hydrocarbon modes. Features from 6 to 7 μm, 9 to 10 μm, and 12.5 μm appear in the ZnSe and the KRS-5 spectra. These features could also, in part, be associated with the input-beam nonuniformity's interacting with residual sphere spatial nonuniformity. In this way, the spectral structure that is due to the beam splitter and the detector can be observed in the results, thus comprising a component of measurement error. Conclusive results will require further characterization.

The indirectly measured absorptance levels in Figs. 7(a)–7(d) over the spectral ranges cited above can be interpreted as arising from cumulative measurement error. The results exhibit an absolute level of error ranging from 0 to 0.002 for the structureless spectral regions up to a maximum of 0.004, at which a structure is observed.

The evaluation of measurement error (by use of the zero-absorptance level) for reflectance of the transparent materials can be transferred with confidence to the opaque sample case (for which a zero-absorptance test is not feasible). An example is a Au mirror reflectance measurement, shown in Fig. 8. In the opaque sample case, there is only a single reflection, whereas for the transparent sample case, multiple reflections contribute to the reflectance result. The higher-order reflected beams will be displaced (because of the angle of incidence), enlarged (because of focus shift), and perhaps deviated (because of sample wedge). Hence the effects of spatial nonuniformity of the sphere throughput will be smaller for the opaque mirror measurement, resulting in a smaller relative measurement uncertainty for the sample reflectance. This is corroborated by the relative lack of spectral structure below 16 μm in the Au mirror reflectance in Fig. 8 (the structure above 16 μm is due to the increased noise level at the extreme end of the detector's spectral range).

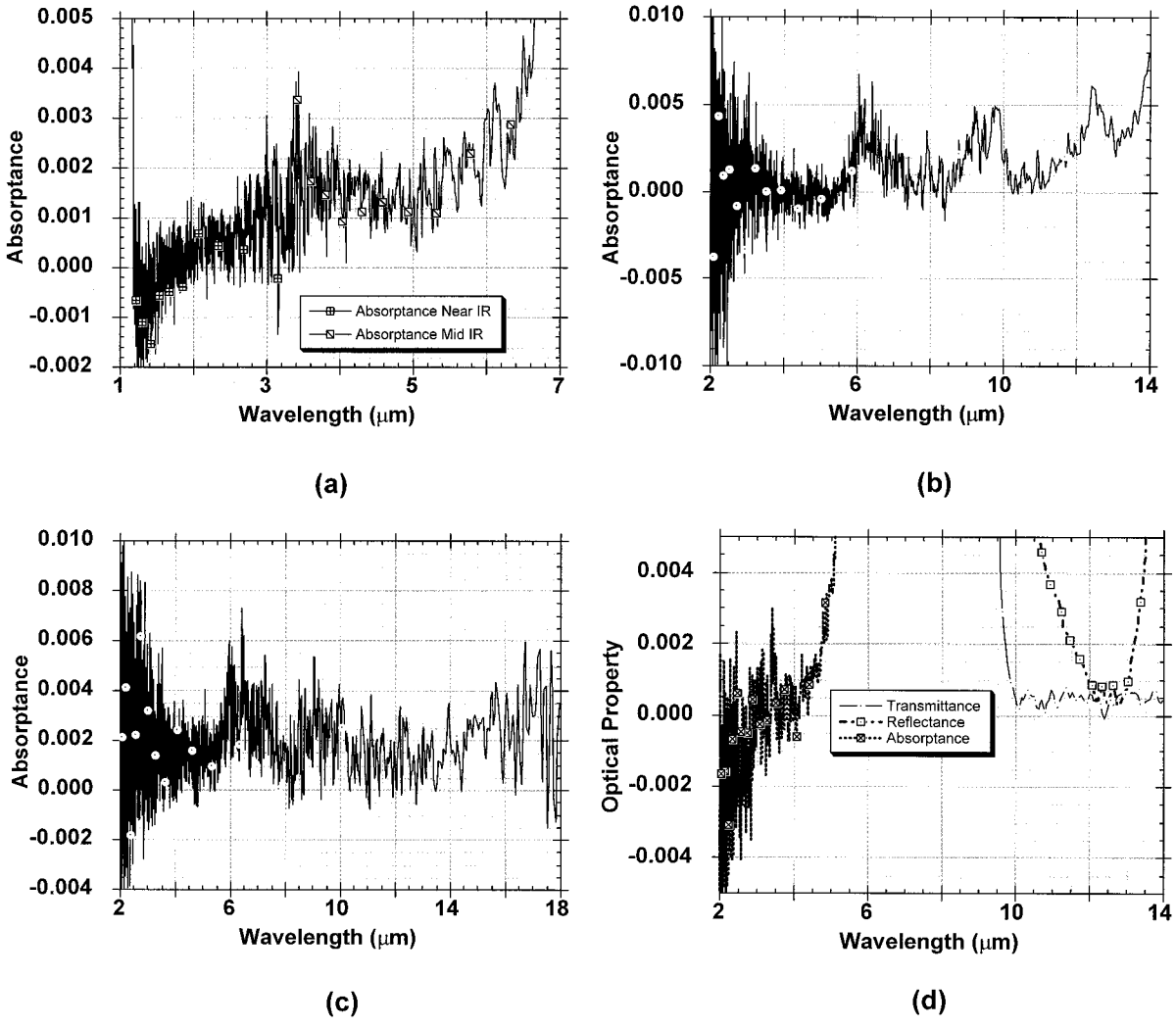

Fig. 7. Expanded plot of spectra shown in Fig. 6, highlighting regions with absorptance near zero: (a) Si, (b) ZnSe, (c) KRS-5, (d) MgF_2. The spectra, in regions where k should be negligible,[12] result from a combination of (1) cumulative measurement error from all sources in transmittance and reflectance, and (2) additional absorption that is due to volume or surface contaminants such as hydrocarbons and water. The MgF_2 spectrum also shows regions of near-zero transmittance and reflectance at longer wavelengths.

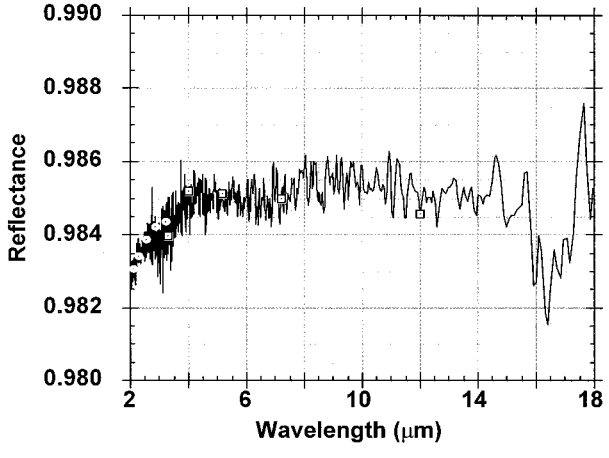

Fig. 8. Au electroplated mirror reflectance. The spectrum is a combination of near-IR (2–3.5 μm, circles) and mid-IR (3.5–18 μm, squares) spectra taken with different source–beam-splitter combinations of the FTIR. This accounts for the reduced noise near 2 μm in comparison with Fig. 6.

7. Discussion and Conclusions

The benefits of using the integrating sphere for more accurate detection of light are used in the design and the development of a device for absolute measurement of transmittance, reflectance, and absorptance of specular samples. The method is demonstrated in the case of IR windows and mirror characterization. The ability to measure both transmittance and reflectance in the same geometry is used to quantify directly the total measurement error for nonabsorbing spectral regions, thereby also obtaining reliable uncertainty values for results outside these regions.

On careful study and consideration, it can be observed that use of the integrating sphere significantly reduces several important sources of measurement error, enabling the levels of accuracy demonstrated in this paper. These error sources include sample–detector and detector–interferometer interreflections, detector nonlinearity, detector spatial nonuniformity, and sample–

beam geometry interaction (beam deviation, deflection, and focus shift).[11]

The integrating-sphere system is not suitable for high-sample-throughput applications. For these applications other instrumentation designed for fast relative measurements can be used. Such instruments, in turn, can be calibrated with transfer standard samples that are characterized with the sphere system. This approach has allowed us to improve the accuracy of measurements made on all our FTS instrumentation,[9] including those designed for variable sample temperature and variable incidence-angle characterization, not directly feasible with the sphere system.

For accurate characterization of specular samples, direct mounting onto the sphere is not an absolute requirement. Effective systems have been built, especially for the UV–visible–near-IR spectral region, that incorporate integrating spheres with detector(s) in the standard averaging mode. However, there are at least two important advantages of mounting the sample directly onto the sphere as shown in this paper. Both of these relate to the characterization of nonideal samples. The first is that this design can better handle the worst samples and allow for the greatest amount of beam deflection, deviation, distortion, and focus shift. The second is that one can measure samples that are not perfectly specular, but that also exhibit some degree of scatter. The sphere measurement is a hemispherical measurement and will collect all or most of the scattered light in addition to the specular component.[14] Through use of a compensating wedge to achieve normal incidence on the sample, for reflectance, and the sphere oriented in the position of Fig. 3(b) for transmittance, supplementary measurements can be made to sort out the scattered component from the specular. For important IR window materials, such as ZnS and chemical-vapor-deposited diamond, some scatter is unavoidable and typically is wavelength dependent. The ability to detect and evaluate scattered light is important in understanding IR materials, in quantifying their behavior, and in determining how they can be used appropriately in optical systems.

The sphere system and method presented in this paper is one that can be reasonably easily reproduced and implemented on, or adapted to, most FTIR spectrophotometers in near- to far-IR regions. In addition, the method can be readily implemented in the UV–visible–near-IR regions for use with monochromator instrumentation. A duplicate system of the one described herein would entail a moderate cost. A less expensive version with a simpler rotation stage mechanism and detector arrangement, smaller sphere, etc., although perhaps not yielding the highest accuracy results (approaching 0.1–0.3%), should, if well designed, be expected to produce consistently measurements with uncertainties of the order of 1%. This expectation is reasonable because many of the inherent benefits of using the sphere would remain, even for a simpler version. Such uncertainty levels would compare favorably with most, if not all, commercial accessories currently available. At the same time, improvements to the current sphere system, including the development and the application of a more spatially uniform coating, should result in better performance and potentially higher-accuracy data.

References

1. D. Sheffer, U. P. Oppenheim, and A. D. Devir, "Absolute reflectometer in the mid-infrared region," Appl. Opt. **29,** 129–132 (1990).
2. "Absolute methods for reflection measurement," CIE Tech. Rep. 44 (CIE, Vienna, 1979).
3. J. M. Palmer, "The measurement of transmission, absorption, emission, and reflection," in *Handbook of Optics* (American Institute of Physics, New York, 1997), Vol. II.
4. K. A. Snail, A. A. Morrish, and L. M. Hanssen, "Absolute specular reflectance measurements in the infrared," in *Materials and Optics for Solar Energy Conversion and Advanced Lighting Technology*, S. Holly and C. M. Lampert, eds., Proc. SPIE **692,** 143–150 (1986).
5. T. M. Wang, K. L. Eckerle, and J. J. Hsia, "Absolute specular reflectometer with an autocollimator telescope and auxiliary mirrors," NIST Tech. Note 1280 (U.S. Government Printing Office, Washington, D.C., 1990).
6. F. J. J. Clarke, "Infrared regular reflectance standards from NPL," in *Developments in Optical Coatings*, I. Ried, ed., Proc. SPIE **2776,** 184–195 (1996).
7. D. B. Chenault, K. A. Snail, and L. M. Hanssen, "Improved integrating-sphere throughput with a lens and nonimaging concentrator," Appl. Opt. **34,** 7959–7964 (1995).
8. L. M. Hanssen and S. G. Kaplan, "Infrared diffuse reflectance instrumentation and standards at NIST," Anal. Chim. Acta **380,** 289–302 (1999).
9. S. G. Kaplan and L. M. Hanssen, "Infrared regular reflectance and transmittance instrumentation and standards at NIST," Anal. Chim. Acta **380,** 303–310 (1999).
10. J. R. Birch and F. J. J. Clarke, "Fifty sources of error in Fourier transform spectroscopy," Spectrosc. Eur. **7,** 16–22 (1995).
11. S. Kaplan, R. U. Datla, and L. M. Hanssen, "Testing the radiometric accuracy of Fourier transform transmittance measurements," Appl. Opt. **36,** 8896–8908 (1997).
12. E. O. Palik, *Handbook of Optical Constants of Solids* (Academic, San Diego, Calif., 1985).
13. P. Klocek, *Handbook of Infrared Optical Materials* (Wiley, New York, 1991).
14. L. M. Hanssen and S. G. Kaplan, "Problems posed by scattering transmissive materials for accurate transmittance and reflectance measurements," in *Optical Diagnostic Methods for Inorganic Transmissive Materials*, R. U. Datla and L. M. Hanssen, eds., Proc. SPIE **3425,** 28–36 (1998).